ACS Medicinal Chemistry Letters

Letter

Cite This: ACS Med. Chem. Lett. 2017, 8, 1224−1229

Mtb PKNA/PKNB Dual Inhibition Provides Selectivity Advantages for Inhibitor Design To Minimize Host Kinase Interactions

Tiansheng Wang,*[,†] Guy Bemis,[†] Brian Hanzelka,[†,§] Harmon Zuccola,[†] Michael Wynn,[†] Cameron Stuver Moody,[†] Jeremy Green,[†] Christopher Locher,[†,∥] Aixiang Liu,[‡] Hongwu Gao,[‡] Yuzhou Xu,[‡] Shaohui Wang,[‡,⊥] Jie Wang,[‡] Youssef L. Bennani,[†] John A. Thomson,[†,#] and Ute Müh[†,▽]

[†]Vertex Pharmaceuticals Incorporated, 50 Northern Avenue, Boston, Massachusetts 02210, United States

[‡]Shanghai ChemPartner Co. Ltd., 998 Halei Road, Pudong New Area, Shanghai 201203, China

Supporting Information

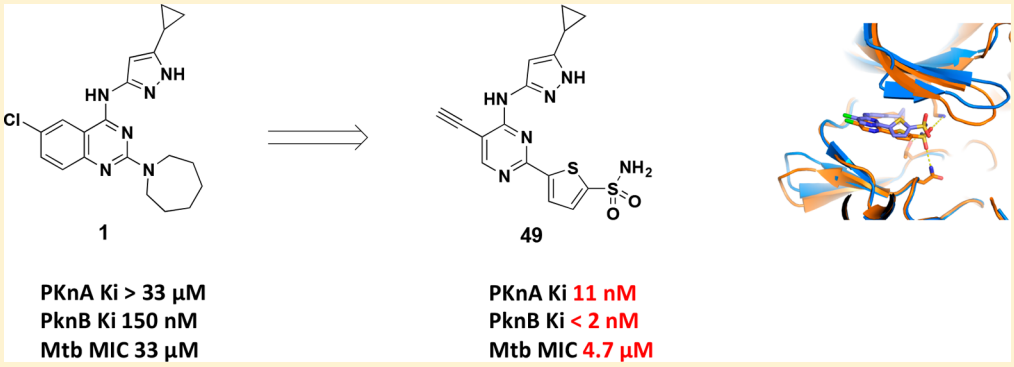

ABSTRACT: Drug resistant tuberculosis (TB) infections are on the rise and antibiotics that inhibit *Mycobacterium tuberculosis* through a novel mechanism could be an important component of evolving TB therapy. Protein kinase A (PknA) and protein kinase B (PknB) are both essential serine-threonine kinases in *M. tuberculosis*. Given the extensive knowledge base in kinase inhibition, these enzymes present an interesting opportunity for antimycobacterial drug discovery. This study focused on targeting both PknA and PknB while improving the selectivity window over related mammalian kinases. Compounds achieved potent inhibition ($K_i \approx 5$ nM) of both PknA and PknB. A binding pocket unique to mycobacterial kinases was identified. Substitutions that filled this pocket resulted in a 100-fold differential against a broad selection of mammalian kinases. Reducing lipophilicity improved antimycobacterial activity with the most potent compounds achieving minimum inhibitory concentrations ranging from 3 to 5 μM (1−2 μg/mL) against the H37Ra isolate of *M. tuberculosis*.

KEYWORDS: *Protein kinase A (PknA), protein kinase B (PknB), Mycobacterium tuberculosis, dual targeting, structure activity relationship (SAR)*

Tuberculosis (TB) remains a major unmet medical need due to widespread drug resistance, HIV coinfection, and ineffective healthcare management with approximately two billion latent infections, ten million new cases, and two million deaths each year.[1] Antibacterial compounds that act through a novel mechanism of inhibition may offer advantages to treat infections with drug-resistant strains. Of the 11 serine/threonine (Ser/Thr) protein kinases described in *Mycobacterium tuberculosis* (Mtb),[2,3] protein kinase A (PknA) and protein kinase B (PknB) are especially attractive drug targets because they are essential for bacterial growth both in culture medium and in Mtb-infected host macrophages.[4−6] The availability of protein crystal structures for PknB[7−9] will enable the design of potent and selective compounds. PknA and PknB are crucial for cell wall formation, resuscitation from dormancy, and performing multiple regulatory functions in metabolism and adaptation to environmental stress.[10−13] Antimycobacterial activity through PknB inhibition has been explored by others.[14,15] However, only moderate antibacterial activity was achieved, and no data on PknA was reported. We expand on these results by targeting both PknA and PknB. Dual targeting has the potential to significantly lower the frequency at which resistance develops. However, broadening the inhibitor specificity may increase the risk of introducing adverse side effects through the inhibition of mammalian kinases. We report here the optimization of a lead series that achieved potent inhibition of both PknA and PknB with K_i values in the single digit nanomolar range. Structures of compound-enzyme cocrystals allowed the identification of a unique feature in the binding site of PknB. Compound substitutions that exploit this feature achieved a 100-fold selectivity window over a range of mammalian kinases. For

Received: July 5, 2017
Accepted: November 28, 2017
Published: November 28, 2017

DOI: 10.1021/acsmedchemlett.7b00239
ACS Med. Chem. Lett. 2017, 8, 1224−1229

Scheme 1. Diversification Strategy and Initial Quinazoline SAR

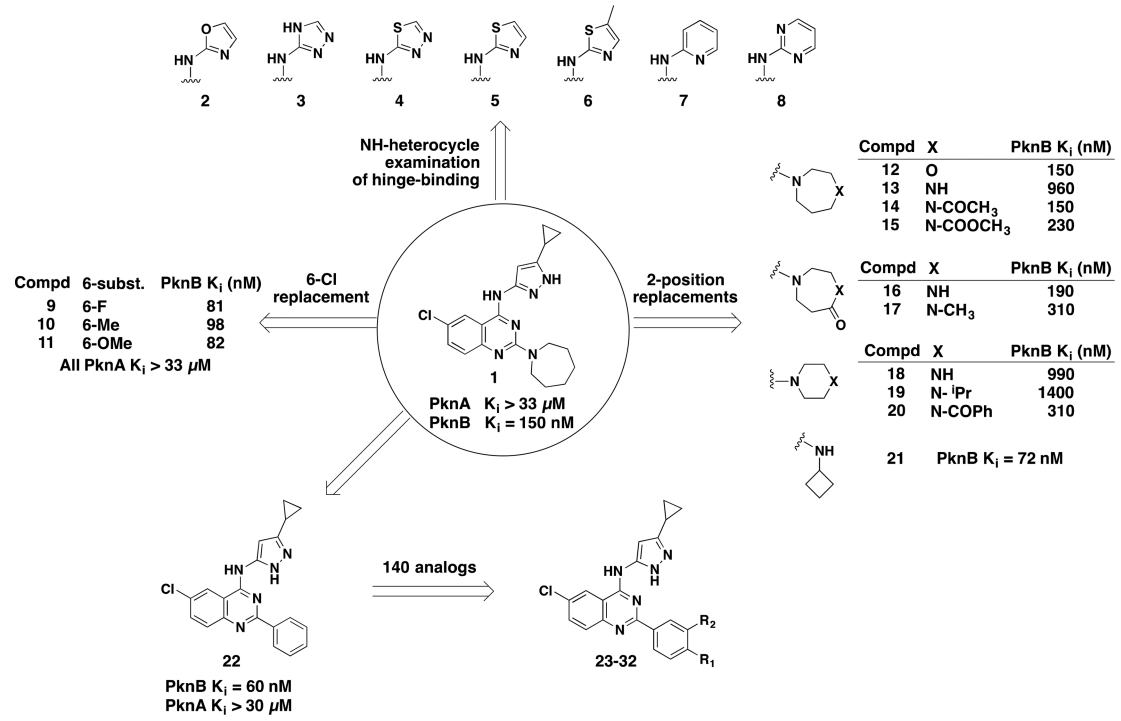

many of the lead compounds, improved enzymatic potency translated to improved antimycobacterial activity. Several compounds achieved a minimum inhibitory concentration (MIC) around 3−5 μM (1−2 μg/mL).

The project was initiated by screening a collection of 1078 compounds representing kinase inhibitor chemical diversity against the PknA and PknB kinase domains. Compounds with K_i < 10 μM were modeled into the active site of PknB in complex with phosphomethylphosphonic acid adenylate ester (PDB ID: 1O6Y)[9] and into a homology model of PknA to get an approximation of dual targeting. Hit compounds that were able to dock into both sites with similar poses and reasonable strain energies were prioritized for follow-up. Quinazoline **1** was selected as our starting point because it showed relatively strong PknB inhibition (K_i = 150 nM) and a good MIC against Mtb H37Ra (33 μM). Although **1** did not show inhibition of PknA, the sequence similarity between PknA and PknB (43% identity in the kinase domains; 56% identical in the ATP binding pocket) made it likely that we would be able to build in inhibition for both isoforms.

Scheme 1 summarizes the diversification strategy used for quinazoline **1**. Since 4-(aminopyrazolyl)-substituted quinazolines inhibit several mammalian host kinases as well as Mtb kinases by binding to the hinge region, we wanted to identify

Table 1. Representative PknA and PknB Enzyme Inhibition (K_i): SAR of 2-Aryl-Substituted Quinazolines

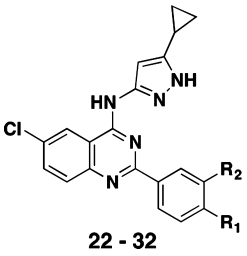

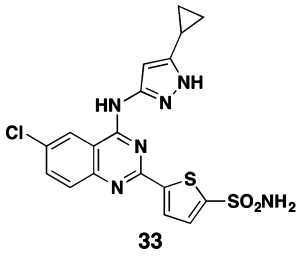

compd	R_1	R_2	PknB K_i (nM)	PknA K_i (nM)
23	CH_2CN	H	5	>4000
24	H	CH_2CN	38	ND
25	H	CN	50	>4000
26	H	$CONH_2$	15	>4000
27	H	CH_2OH	23	2300
28	CH_2CONH_2	H	23	1800
29	$CONH_2$	H	29	>4000
30	CN	H	88	>4000
22	H	H	69	>4000
31	SO_2NH_2	H	24	22
32	H	SO_2NH_2	**6**	**<8**
33			**<1**	**<8**

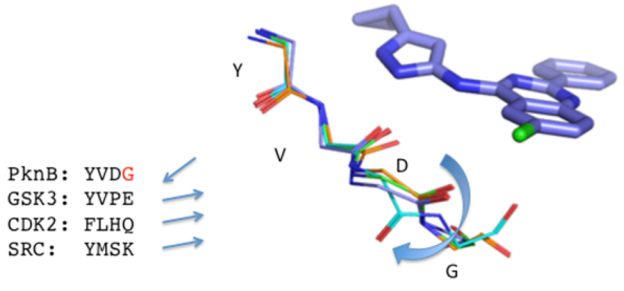

Figure 1. Compound **22** docked into the ATP binding site of PknB, and the mammalian kinase GSK3β, CDK2, and SRC. Labels identify PknB residue numbers corresponding to cyan structure. For clarity, amino acid side chains are not shown. Straight arrows indicate the direction of the C═O bond between the 3rd and 4th residues in the sequences shown, and the curved arrow indicates flipping of the peptide bond between D and G residues. Alignment was done using C-alpha atoms. Red G is the residue that allows PKnB to undergo conformational change.

DOI: 10.1021/acsmedchemlett.7b00239
ACS Med. Chem. Lett. 2017, 8, 1224−1229

Table 2. 6-Substituted Quinazoline with Host Kinase Selectivity

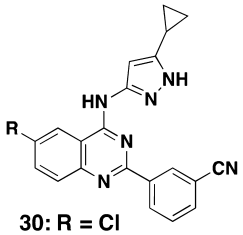

30: R = Cl
34: R = H

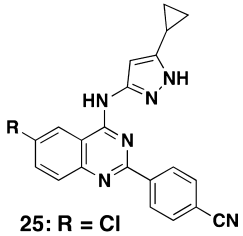

25: R = Cl
35: R = H

	compd			
kinase K_i (nM)	**34**	**30**	**35**	**25**
PknB	40	88	46	50
GSK3β	9	190	70	>4000
CDK2	11	170	140	750
SRC	22	710	18	200

alternative hinge-binding elements in order to obtain selectivity. We synthesized an extensive set of amino heterocyclic replacements for the amino-pyrazole, including oxazole (**2**), triazole (**3**), thiadiazole (**4**), thiazole (**5**, **6**), pyridine (**7**), and pyrimidine (**8**). Unfortunately, all these compounds had reduced PknB inhibition. Our hypothesis is that these compounds destabilized the preferred binding tautomer (in the case of the triazole), removed a key Ar−H interaction (in the case of the thiadiazole), or disturbed the overall geometry of interaction with the kinase hinge area (in the cases of pyridine and pyrimidine).

A small structure−activity relationship (SAR) study of the 6-position, replacing Cl with F (**9**), methyl (**10**), and methoxy (**11**), showed that it was possible to maintain PknB activity at this position with a variety of substituents, an opportunity that was later exploited for selectivity and cell-based activity (see below).

Next, an investigation of the quinazoline 2-position was conducted. One of our goals was to preserve the sp^3 character of the azepane substituent, if possible, to retain more drug-like physicochemical properties.[16] The neutral oxazepane analog **12** had an unchanged PknB K_i of 150 nM, but when a positive charge was introduced with the diazepane analog **13**, we observed a six-fold loss of activity. Acylation of the amine to return it to the neutral state as either the amide or carbamate analog (**14** and **15**) recapitulated the original PknB potency of 150 and 230 nM, respectively. In accord with this developing SAR, the diazepanone analogs **16** and **17** also gave PknB K_i potencies of 190 and 310 nM, respectively. Contraction of the diazepane ring to the six-membered piperazine rings (**18** and **19**) gave weaker activity, but surprisingly so did the acylated version found in **20**. We surmise that the much larger volume of the *N*-benzoyl group was responsible for its diminished activity.

To follow up on this result, a library of 48 amine compounds that were substituted at the quinazoline C2 position was generated. We selected a set of primary and secondary amines containing one or fewer aromatic rings, with the following constraints: MW < 200, PSA < 55 Å, and calculated logP < 2.5. Library members were found to have PknB K_i values ranging from >4 μM to <100 nM. The cyclobutylamino analog (**21**) was the most potent PknB inhibitor (K_i = 72 nM), while most of the other C2-amino analogs plateaued at approximately 100 nM PknB K_i without further improvement. These findings are summarized in Scheme 1.

In addition to our sp^3-retaining C2-substitution strategy, we also explored aryl C2 substitutions. Starting from the baseline 2-phenyl analog (**22**: PknB K_i = 60 nM), we prepared approximately 140 other substituted 2-phenyl analogs. Substituents at the *m*- and *p*-position of the 2-phenyl ring offered excellent PknB potency, but showed no PknA activity. Table 1 shows SARs for a representative set of quinazoline 2-substituted phenyl compounds. The 4-cyanomethylphenyl analog **23** had a PknB K_i of 5 nM, while the 3-cyanomethylphenyl analog **24** had a PknB K_i of 38 nM. Additional polar functionalities such as 4-cyano (**25**), 4-$CONH_2$ (**26**), and 4-hydroxymethyl (**27**) were examined, and additional 3-substituted analogs were made such as 3-acetamide **28** (K_i = 23 nM)), 3-$CONH_2$ **29** (K_i = 29 nM), and cyano **30** (K_i = 88 nM). Overall, the substituted phenyl analogs **24** to **30** maintained similar levels of PknB inhibitory activity compared to their parent phenyl analog **22**. It was not until we prepared the 4-hydroxymethyl (**27**) and 3-acetamide (**28**) compounds that we began to observe inhibition of PknA (2.3 and 1.8 μM, respectively.) Further exploration of the H-bonding substituents at both 3- and 4-positions provided excellent inhibition of PknA and PknB with the primary sulfonamide in either position (compounds **31** and **32**). The 4-SO_2NH_2 analog **31** reached K_i values of 24 and 22 nM for PknB and PknA, respectively. The 3-SO_2NH_2 analog **32** also demonstrated single-digit K_i values (6 and <8 nM) for PknB and PknA. The value of this substituent was further demonstrated when we changed the quinazoline 2-substituent from phenyl to a thiophene ring bearing a 5-sulfonamide group (**33**) and found even more potent dual PknB and PknA inhibition. These findings are summarized in Table 1.

We next investigated opportunities for achieving selectivity over mammalian host kinases. We chose GSK3β, CDK2, and SRC for selectivity assessment since each was known to be inhibited by compounds of this class. Overlay of the PknB hinge binding region with a selection of mammalian host kinases including GSK3β, CDK2, and SRC showed that the area immediately surrounding the 6-chloro substituent of **1** provided a distinct binding pocket that could be exploited for mycobacterial kinase selectivity. As shown in Figure 1, it can be seen that Gly-97 of PknB is "flipped" relative to the corresponding residues of the mammalian kinases, such that the backbone carbonyl of the adjacent residue, Asp-96, is pointed away from the inhibitor, creating additional space that accommodates the 6-Cl of **22**.

To further substantiate the Mtb PknB selectivity of inhibitory compounds over mammalian kinases, 6-Cl quinazoline analogs were compared with 6-H compounds as summarized in Table 2. As predicted, we found similar PknB potency for both 6-Cl and 6-H quinazolines (**34** vs **30** and **35** vs **25**, respectively), while inhibition of the three mammalian kinases was reduced 5−50-fold with the 6-Cl compounds (**30** and **25**).

Thus far, we had been able to improve enzyme potency and selectivity for the quinazoline series. However, we were unable to improve antimycobacterial activity since, despite lowering PknB inhibition roughly 100-fold, the MIC against Mtb H37Ra remained at 33 μM or higher. It is possible that our inhibitors failed to penetrate the Mtb cell wall, or they were subject to rapid efflux.

Some antibacterial compounds can cross the bacterial cell wall through channel-forming porins that enable the diffusion of small, hydrophilic solutes.[17] Efflux pumps, while not well studied in Mtb, tend to be particularly active on lipophilic substrates. Hence, reducing lipophilicity can be a successful strategy both for

DOI: 10.1021/acsmedchemlett.7b00239
ACS Med. Chem. Lett. 2017, 8, 1224−1229

Scheme 2. Compounds 36−38 and 46−49 and the Representative Syntheses of 37, 38, and 49

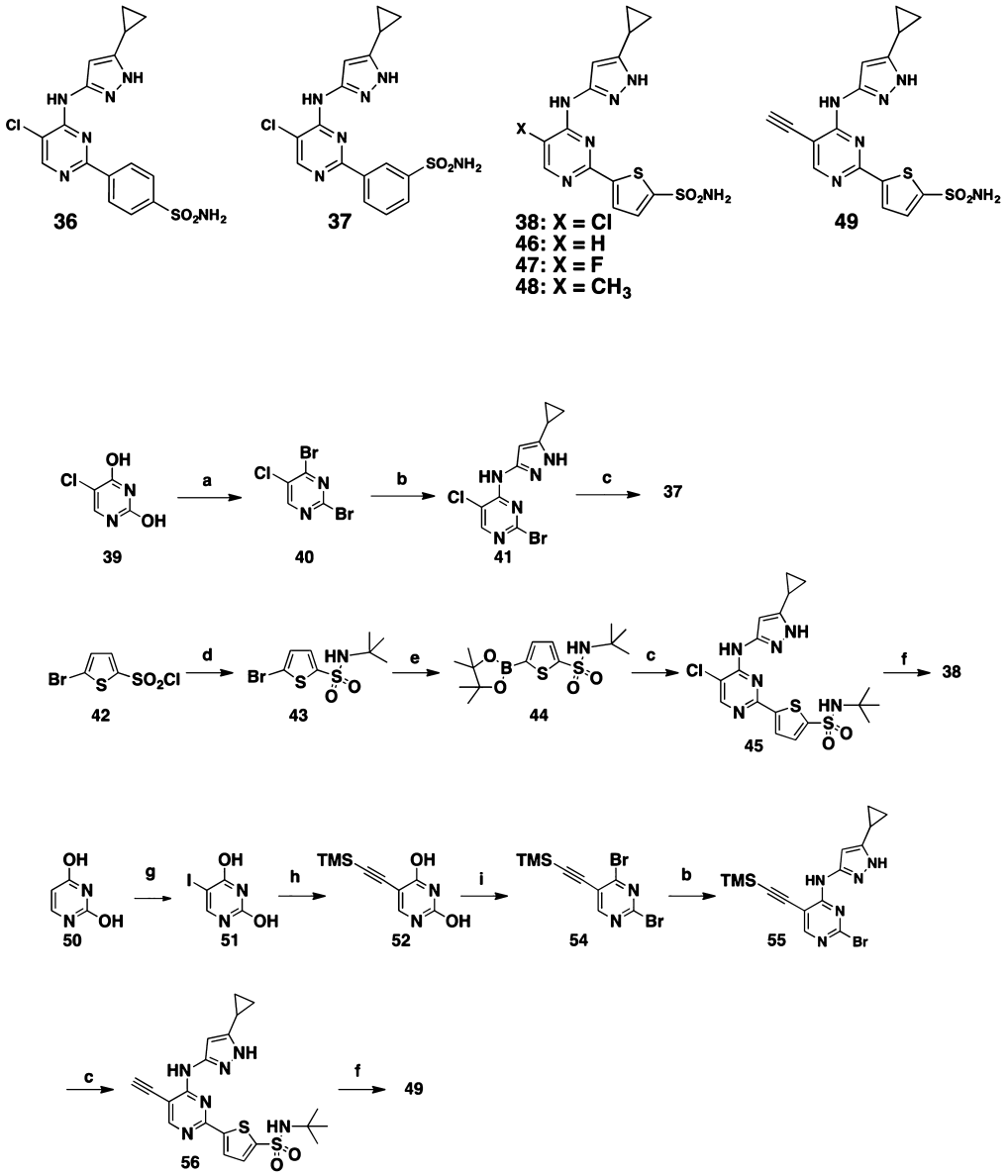

[a] *N*,*N*-Dimethylaniline (2 equiv), $POBr_3$ (3 equiv), toluene, 90 °C, 2 h, 83%. [b] 5-Cyclopropyl-1*H*-pyrazol-3-amine, EtOH, RT, 4 h, 78%. [c] 3- or 4-(Pinacolatoboranyl)-benzenesulfonamide for **36** and **37**, or **44** for **38** and **56**, Pd(dppf)Cl_2 (0.1 equiv), Na_2CO_3 (4 equiv), dioxane/H_2O (4:1), 100 °C, 15 h. [d] *t*-Butylamine, dioxane, 20 °C, 4 h, 94%. [e] Bis-pinacolatodiboron (1.2 equiv), Pd(dppf)Cl_2 (0.1 equiv), CH_3COOK (4.0 equiv), dioxane, 100 °C, 3 h, 70%. [f] BCl_3, DCM, 20 °C, 6 h. [g] NIS, AcOH, RT, 7 h, 95%. [h] TMS-acetylene (1.2 equiv), $(Ph_3P)_2PdCl_2$ (0.25 equiv), CuI (0.25 equiv), EtOAc, RT, 4 h, 46%. [i] *N*,*N*-Dimethylaniline, $POBr_3$, 100 °C, 50 min, toluene, 51%.

Table 3. Enzyme Inhibition and MIC (μM) of Pyrimidines against *Mycobacterium tuberculosis*

compd	PknB K_i (nM)	PknA K_i (nM)	Mtb MIC (μM)
36	13	2900	>100
37	17	<8	8.3
38	<1.3	9	6.25
46	4	18	4.2
47	<1	12	3.1
48	4	18	4.7

improving permeability through the bacterial cell wall and for avoiding efflux. We set about reducing the lipophilicity of our most potent kinase inhibitors while also minimizing their size. Similar to the approach described by Chapman et al.,[14] we truncated the quinazoline ring into a simple monocyclic pyrimidine ring. In addition, we incorporated the sulfonamide substituent to provide potent PknA inhibition. Toward this objective, we synthesized the pyrimidine analogs **36**, **37**, and **38** (Scheme 2). The preparation of **37** and **38** is described in Scheme 2. Treatment of 5-chloropyrimidine-2,4-diol (**39**) with $POBr_3$ gave the 2,4-dibromo-5-chloro-pyrimidine (**40**), which reacted with 5-cyclopropyl-1*H*-pyrazol-3-amine to afford **41**. Suzuki coupling of **41** with 3-(4,4,5,5-tetramethyl-1,3,2-dioxaborolan-2-yl)benzene-sulfonamide then produced target compound **37**. For **38**, the synthesis started with the reaction of 5-bromothiophene-2-sulfonyl chloride (**42**) with 2-methylpropan-2-amine to form 5-bromo-*N*-(*tert*-butyl)thiophene-2-sulfonamide (**43**), which then was converted to the pinacol-boron

DOI: 10.1021/acsmedchemlett.7b00239
ACS Med. Chem. Lett. 2017, 8, 1224−1229

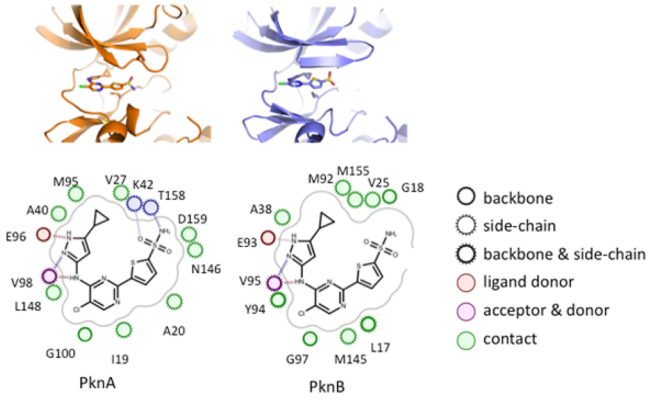

Figure 2. Compound **38** bound to PknA (left) and PknB (right), and with key amino acid residues that interact with **38**.

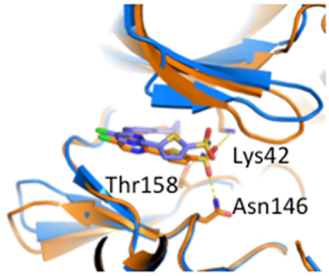

Figure 3. X-ray crystal structures for **38** complexed to PknA (orange) and PknB (blue.) Structures were overlaid using PyMol for alignment. Dotted lines represent close polar contacts discussed in the text.

Table 4. Selectivity of PknB Inhibitors with Reduced Inhibition of the Mammalian Kinase CDK2

compd	PknB K_i (nM)	PknA K_i (nM)	CDK2 K_i (nM)	selectivity
46	4	18	7	2
38	<1.3	9	17	>13
49	<2	11	147	>74

ester **44**. Suzuki coupling, followed by removal of the *t*-butyl group with BCl_3 provided **38**.

Each of the three sulfonamide analogs **36**, **37**, and **38** were potent PknB and PknA inhibitors, while **37** and **38** demonstrated single-digit micromolar MIC against Mtb H37Ra. Additional 5-substituted pyrimidine analogs **46**, **47**, and **48** were prepared and all showed excellent PknB and PknA potency that translated to improved Mtb H37Ra MIC values (Table 3).

To confirm our proposed binding modes and to understand the SAR observed for PknA and PknB, we used X-ray crystallography to solve the structure of compound **38** complexed with PknA and also complexed with PknB. Figure 2 shows that the aminopyrazole provides the key hinge-binding interactions, with the cyclopropyl group interacting in the small hydrophobic pocket provided by Met95 and Val27 in PknA and by the analogous residues Met92 and Val25 in PknB. These structures also provide some clues to understanding why the SO_2NH_2 group provides enhanced inhibition of PknA. The $-SO_2NH_2$ group bound to PknA shows three relatively close polar contacts, to the side chains of Lys42, Thr158, and Asn146 (Figure 3).

We then investigated the C5-position on the pyrimidine ring to determine if we could again exploit the "flipped glycine" pocket for selectivity over mammalian kinases. Toward this effort, the 5-acetylenyl compound **49** was made as shown in Scheme 2. The 5-H analog **46** only showed two-fold selectivity versus CDK2, while the 5-Cl compound **38** gave at least a 15-fold improvement in Mtb PknB selectivity vs CDK2. The sterically more demanding 5-acetylenyl compound **49** demonstrated greater than 100-fold selectivity vs CDK2, with increased PknB potency (Table 4) while maintaining Mtb H37Ra MIC at 4.7 μM.

Finally, we wanted to demonstrate a clear link between kinase inhibition and the observed antimycobacterial activity. For this purpose, we designed the *N*-methyl version of compound **48**, where the kinase hinge-binding nitrogen is blocked. Compound **57** was synthesized as shown in Scheme 3. The starting material 5-cyclopropyl-1-methyl-1*H*-pyrazol-3-amine **58** was prepared from simple methylation of 3-cyclopropyl-1*H*-pyrazol-5-amine. Reaction with 2,4-dibromo-5-methylpyrimidine followed by Suzuki coupling with intermediate **44** and *N*-*t*-butyl removal gave compound **57**. Consistent with our expectations, compound **57** lost both PknA and PknB enzyme activities (K_i both >4 μM) as well as antimycobacterial activity (Mtb H37Ra MIC > 100 μM).

In conclusion, starting from a 1078-compound screen of a focused collection of diverse kinase-inhibitory compounds, we identified a weak and nonselective quinazoline-based inhibitor of PknB with a quinazoline core that lacked activity against PknA and showed weak antimycobacterial activity. We successfully optimized this series to achieve potent, dual-targeting inhibitors with activity against both PknB and PknA. We identified a structural pocket unique to the mycobacterial kinases that we exploited for two related but distinct series. Compound modifications that filled this pocket gave a significant selectivity window over mammalian kinases. Reducing compound lipophilicity (for example, quinazoline **33** has a calculated logP of 4.1, while for the analogous pyrimidine **38**, 2.7) greatly improved

Scheme 3. Synthesis of 57

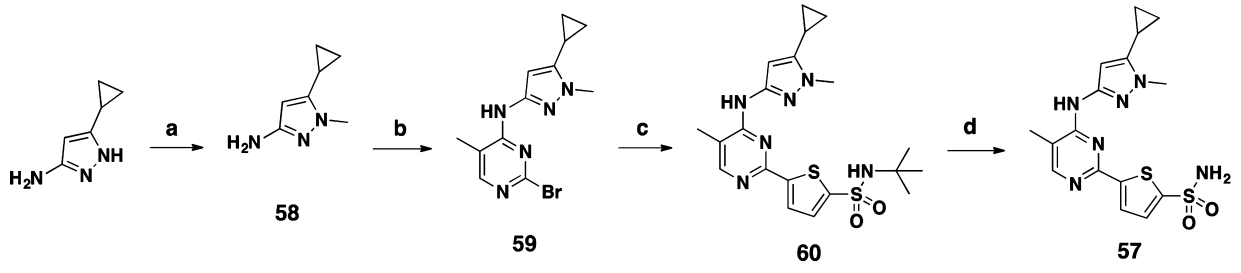

[a] *t*-BuOK, 18-*crown*-6, CH_3I, Et_2O, 0 °C, 3 h, 43%. [b] 2,4-Dibromo-5-methylpyrimidine, EtOH, RT, 8 h, 70%. [c] **44**, $Pd(dppf)Cl_2$ (0.1 equiv), Na_2CO_3 (4 equiv), dioxane/H_2O (4:1), 100 °C, 15 h, 28%. [d] BCl_3, DCM, RT, 30 min, 71%.

DOI: 10.1021/acsmedchemlett.7b00239
ACS Med. Chem. Lett. 2017, 8, 1224−1229

the antibacterial activity, with the best compounds in the series active against Mtb H37Ra with MIC in the range of 3−5 μM (1−2 μg/mL) and potency commensurate with clinically used antibiotics. Thus, pending further lead optimization efforts, kinase inhibition could be a valuable approach to the discovery of much needed new TB therapeutics.

■ ASSOCIATED CONTENT

Supporting Information

The Supporting Information is available free of charge on the ACS Publications website at DOI: 10.1021/acsmedchemlett.7b00239.

Preparation of all final compounds, kinase and MIC data, PknA and PknB expression, biological assay protocols, and crystallization conditions (PDF)
Spectra of compounds (PDF)

Accession Codes

PDB codes for the X-ray crystal structures described in this study have been deposited in the PDB under the accession codes 6B2P (PknA) and 6B2Q (PknB).

■ AUTHOR INFORMATION

Corresponding Author

*E-mail: tiansheng_wang@vrtx.com. Phone: 617-341-6484.

ORCID

Tiansheng Wang: 0000-0001-5073-2670
Jeremy Green: 0000-0003-4544-6412

Present Addresses

[§]Hennessy Research Associates, 12700 Johnson Drive, Shawnee, Kansas 66216, United States. E-mail: bhanzelka@hennessyresearch.com.
[∥]Versatope Therapeutics, MassChallenge Design and Innovation Center, 21 Drydock Lane, Boston, Massachusetts 02210, United States. E-mail: Christopher.locher@versatope.com.
[⊥]GlaxoSmithKline R&D China, No. 3 Building, 898 Halei Road, Shanghai 201203, China. E-mail: shaohui.wang@gsk.com.
[#]P.O. Box 2241, Acton, Massachusetts 01720, United States. E-mail: jtexvertex@yahoo.vom.
[▽]Department of Microbiology, University of Iowa, 51 Newton Road, Iowa City, Iowa 52242, United States. E-mail: ute-muh@uniowa.edu.

Notes

The authors declare no competing financial interest.

■ ACKNOWLEDGMENTS

We would like to express our gratitude to ChemPartner's scientists Jianguo Chen, Xiaoming Li, Zhongtai Piao, and Jingwen Zang for their synthetic (J.C., X.L., Z.P.) and biological (J.Z.) assistance. We thank Barry Davis and Brian Ledford, both of Vertex, for HRMS and NOE studies.

■ ABBREVIATIONS

Mtb, *Mycobacterium tuberculosis*; PknA, Protein kinase A; PknB, Protein kinase B; SAR, structure−activity relationship; GSK 3-beta, glycogen synthase kinase 3 beta; CDK2, cyclin-dependent kinase 2; MIC, minimum inhibitory concentration; PSA, polar surface area

■ REFERENCES

(1) WHO. Global tuberculosis report, 2013.
(2) Av-Gay, Y.; Jamil, S.; Drews, S. J. Expression and characterization of the Mycobacterium tuberculosis serine/threonine protein kinase PknB. *Infect. Immun.* **1999**, *67*, 5676−5682.
(3) Av-Gay, Y.; Everett, M. The eukaryotic-like Ser/Thr protein kinases of Mycobacterium tuberculosis. *Trends Microbiol.* **2000**, *8*, 238−244.
(4) Sassetti, C. M.; Boyd, D. H.; Rubin, E. J. Genes required for mycobacterial growth defined by high density mutagenesis. *Mol. Microbiol.* **2003**, *48*, 77−84.
(5) Sassetti, C. M.; Rubin, E. J. Genetic requirements for mycobacterial survival during infection. *Proc. Natl. Acad. Sci. U. S. A.* **2003**, *100*, 12989−12994.
(6) Fernandez, P.; Saint-Joanis, B.; Barilone, N.; Jackson, M.; Gicquel, B.; Cole, S. T.; Alzari, P. M. The Ser/Thr protein kinase PknB is essential for sustaining mycobacterial growth. *J. Bacteriol.* **2006**, *188*, 7778−7784.
(7) Szekely, R.; Waczek, F.; Szabadkai, I.; Nemeth, G.; Hegymegi-Barakonyi, B.; Eros, D.; Szokol, B.; Pato, J.; Hafenbradl, D.; Satchell, J.; Saint-Joanis, B.; Cole, S. T.; Orfi, L.; Klebl, B. M.; Keri, G. A novel drug discovery concept for tuberculosis: inhibition of bacterial and host cell signalling. *Immunol. Lett.* **2008**, *116*, 225−231.
(8) Young, T. A.; Delagoutte, B.; Endrizzi, J. A.; Falick, A. M.; Alber, T. Structure of Mycobacterium tuberculosis PknB supports a universal activation mechanism for Ser/Thr protein kinases. *Nat. Struct. Biol.* **2003**, *10*, 168−174.
(9) Ortiz-Lombardia, M.; Pompeo, F.; Boitel, B.; Alzari, P. M. Crystal structure of the catalytic domain of the PknB serine/threonine kinase from Mycobacterium tuberculosis. *J. Biol. Chem.* **2003**, *278*, 13094−13100.
(10) Prisic, S.; Dankwa, S.; Schwartz, D.; Chou, M. F.; Locasale, J. W.; Kang, C. M.; Bemis, G.; Church, G. M.; Steen, H.; Husson, R. N. Extensive phosphorylation with overlapping specificity by Mycobacterium tuberculosis serine/threonine protein kinases. *Proc. Natl. Acad. Sci. U. S. A.* **2010**, *107*, 7521−7526.
(11) Chou, M. F.; Prisic, S.; Lubner, J. M.; Church, G. M.; Husson, R. N.; Schwartz, D. Using bacteria to determine protein kinase specificity and predict target substrates. *PLoS One* **2012**, *7*, e52747.
(12) Kang, C. M.; Abbott, D. W.; Park, S. T.; Dascher, C. C.; Cantley, L. C.; Husson, R. N. The Mycobacterium tuberculosis serine/threonine kinases PknA and PknB: substrate identification and regulation of cell shape. *Genes Dev.* **2005**, *19*, 1692−1704.
(13) Ortega, C.; Liao, R.; Anderson, L. N.; Rustad, T.; Ollodart, A. R.; Wright, A. T.; Sherman, D. R.; Grundner, C. Mycobacterium tuberculosis Ser/Thr protein kinase B mediates an oxygen-dependent replication switch. *PLoS Biol.* **2014**, *12*, e1001746.
(14) Chapman, T. M.; Bouloc, N.; Buxton, R. S.; Chugh, J.; Lougheed, K. E.; Osborne, S. A.; Saxty, B.; Smerdon, S. J.; Taylor, D. L.; Whalley, D. Substituted aminopyrimidine protein kinase B (PknB) inhibitors show activity against Mycobacterium tuberculosis. *Bioorg. Med. Chem. Lett.* **2012**, *22*, 3349−3353.
(15) Lougheed, K. E.; Osborne, S. A.; Saxty, B.; Whalley, D.; Chapman, T.; Bouloc, N.; Chugh, J.; Nott, T. J.; Patel, D.; Spivey, V. L.; Kettleborough, C. A.; Bryans, J. S.; Taylor, D. L.; Smerdon, D. J.; Buxton, R. S. *Tuberculosis (Oxford, U. K.)* **2011**, *91*, 277−286.
(16) Lovering, F.; Bikker, J.; Humblet, C. Escape from flatland: increasing saturation as an approach to improvimng clinical success. *J. Med. Chem.* **2009**, *52*, 6752−6756.
(17) Vargas, J. R.; Stanzl, E. G.; Teng, N. N. H.; Wender, P. A. Cell-penetrating, guanidinium-rich molecular transporters for overcoming efflux-mediated multidrug resistance. *Mol. Pharmaceutics* **2014**, *11*, 2553−2565.

DOI: 10.1021/acsmedchemlett.7b00239
ACS Med. Chem. Lett. 2017, 8, 1224−1229